

General Disclaimer

One or more of the Following Statements may affect this Document

- This document has been reproduced from the best copy furnished by the organizational source. It is being released in the interest of making available as much information as possible.
- This document may contain data, which exceeds the sheet parameters. It was furnished in this condition by the organizational source and is the best copy available.
- This document may contain tone-on-tone or color graphs, charts and/or pictures, which have been reproduced in black and white.
- This document is paginated as submitted by the original source.
- Portions of this document are not fully legible due to the historical nature of some of the material. However, it is the best reproduction available from the original submission.

3

"Made available under NASA sponsorship
in the interest of early and wide dis-
semination of Earth Resources Survey
Program information and without liability
for any use made thereof."

NASA CR-

144-5769

E 7.6 - 1 0.1 5.7

Title of Investigation:

Investigation of Environmental Change Pattern in Japan

RECEIVED
NASA STI FACILITY
ACQ. BR. *Jack*

FEB 18 1976

Principal Investigator

Takakazu MARUYASU *nts*

Science University of Tokyo

Noda City, Chiba ken, 278, Japan

DAFF 1019452
1 2 3 4 5

Co Investigator

Hiroaki OCHIAI

Toba Merchant Marine College

Toba City, Mie Ken, 517, Japan

Takamasa NAKANO

Tokyo Metropolitan University

Yagumo, Meguro-ku, Tokyo, Japan

18 December, 1975

FINAL REPORT

(E76-10157) INVESTIGATION OF ENVIRONMENTAL
CHANGE PATTERN IN JAPAN Final Report
(Science Univ. of Tokyo (Japan).) 29 p HC
CSCL 14B G3/43 \$4.00

N76-17466

Name and address of
National Sponcering
Agency

Science and Technology Agency

Kasumigaseki 2-2-1, Chiyodaku,
Tokyo, 100, Japan.

Original photography may be purchased from:
EROS Data Center
10th and Dakota Avenue
Sioux Falls, SD 57198

ORIGINAL CONTAINS
COLOR ILLUSTRATIONS

On the measurement of ground control point
by satellite photographs and its precision

Takakazu Maruyasu

Professor of the Science University of Tokyo

1. Introduction

It has become a common technique now to measure the position on the ground and to make a topographical map using aerial photographs. The flight altitude applied to aerial photogrammetry extends generally from several hundreds meters to ten thousands meters, and an airplane or a helicopter is employed. There are three types of camera used for aerial photographs, ie, usual angle, wide angle and superwide angle, among which wide angle camera is most commonly employed. And the focal length of this camera is 150 mm or 11.5mm. In the case of taking ground photographs by the camera which has 150mm focal length lens from 10 thousands altitude, the photoscale becomes about 1/60000 and this is enough for compiling the topographical map of 1/50000.

Satellite flies higher than an airplane. If the photographs were taken from the altitude of satellite, how precise results could be expected? Proceeding to discuss this point, we must examine whether we could get well-oriented stereophotographs from space.

This report is an approach to these two points

2. Satellite Photographs used for this study

For this work, we selected a pair of good quality photographs among available six pairs which were taken by the multi-band camera S-190B. The focal length of this cameras is 152.4mm, and the picture angle is about 30 degree. Therefore, the size of picture is limited 57x57 mm. As SKYLAB flies about 435km high above the ground, the ground area covered in a picture becomes about 163x163km. And these photographs have 60% overlap each other.

3. Orientation of Satellite Photographs

Whether this satellite photographs could be orientated by usual photogrammetric method is largely depend on the picture

angle of S190A camera. As shown in Fig.1, there are three types of cameras, and among these cameras wide angle camera is most commonly employed. In this camera the picture angle is about 90° . As compared with this camera, picture angle of S190A is only 30° . Although SKYLAB photoes are taken from very high altitude, ground coverage is relatively narrow, and orientation of these photos must be excuted in a small stereo-region. From these reasons, as we easily understand, orientation factors are sensitively affected by subtle vertical parallax. Therefore it is necessary to measure the position of control points with higher precition than in a case of aerial photogrammetry.

However, as we had to use the same stereo-comparator as for usual photogrammetry, it was unavoidable the residual vertical parallax came up always to a few micron.

This is the reason why we firstly took up the problem how we can get more precise orientation data in the case of narrow angle camera on the satellite.

4. Actual Example of the Calculation of Orientation and its result

In order to check above problems, we did the orientation calculation for a pair of color photos which cover the middle part of Kyushu area.

The calculation is only for relative orientation which is abstracted from a aerial trianguration system. Control points are shown by the symbol O on the figure and these points are selected so as to distribute uniformly on the stereo region and consist of clearly identifiable points on the photograph such as bridge, the top of mountain, the corner of river. The value of longitude and latitude of the points were read out from the topographical map (1:50000) in a unit of second, and these values were translated to the national coordinate system II in Kyushu area. Then the precision of the ground coordinate value is approximately assumed $\pm 50m$ on both direction of X and Y.

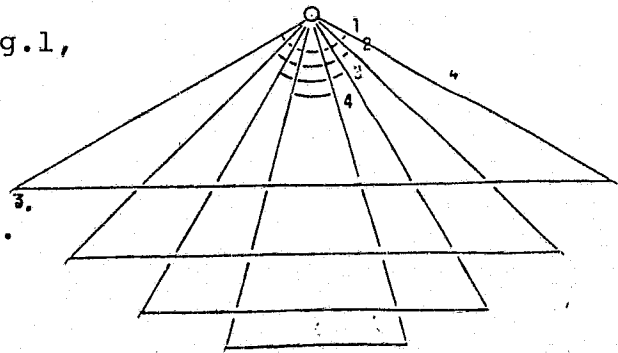


Fig.1 Comparison of Picture Angle of Various Cameras
1:super wide 2:wide 3:narrow 4;S190A

As the intermediate results of calculation, the residual errors of relative orientation were 10 microns by mean square error. This corresponds to the 28m on the ground, because the photo scale is about 1:2,800,000.

The table shows the names of control points, the ground coordinate value measured from the map and calculated using the orientation elements.

The differences of two values are shown. From this results it becomes clear that:

(1) Stereoscopic satellite photos can be orientated by aerial method

(2) In this case, the residual errors of control points are under ± 100 m in XY direction and also 200m in Z direction. Specially we can find the big errors as 600m or 400m in this table, but these are

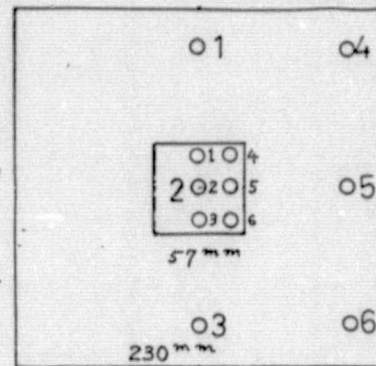
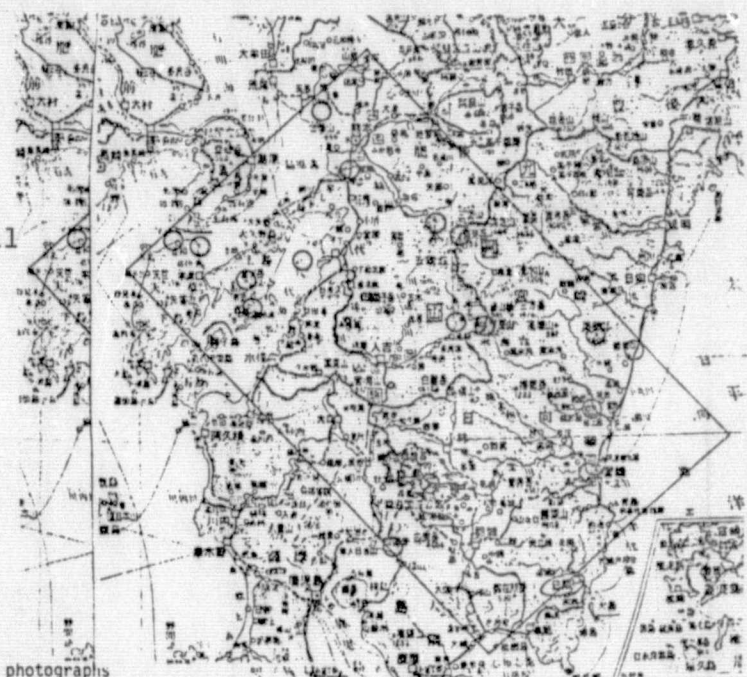


Fig. 2
Comparison of picture size of a aerial photograph and 190A photograph



Orientated results of stereo satellite photographs

Point name	calculated value (km)			Ground control coordinates(km)			Differences of two value (m)		
	X	Y	Z	XB	YB	ZB	DX	DY	DZ
Miyazaki	-121.747	39.898	0.125	-121.635	39.931	0.001	-111	-33	124
Takachiho	-123.976	-7.277	1.444	-123.897	-7.436	1.574	-79	159	-130
Dairo-ike	-119.878	-13.997	1.259	-119.887	-13.606	1.411	9	-391	-152
Kenko-kawa	-144.185	-20.217	0.018	-144.019	-20.088	0.000	-166	-129	17
Tsuji-shima	-49.984	-82.287	0.294	-49.924	-82.510	0.000	-60	223	294
Kame-shima	-50.832	-75.216	-0.107	-50.874	-75.316	0.000	42	100	-107
Mae-shima	-71.855	-60.029	0.036	-71.798	-60.179	0.000	-58	150	36
Kura-take	-63.715	-65.551	0.678	-63.617	-63.134	0.682	-98	-418	-4
Hako-shima	-57.759	-46.844	-0.194	-57.823	-46.964	0.000	64	120	-194
Ichifusa-dam	-75.542	2.163	0.354	-75.549	2.171	0.399	7	-8	-45
Ichifusa-yama	-76.560	9.852	1.807	-76.684	9.756	1.721	124	96	86
Hitotsuse-hashi	-104.942	42.172	0.237	-104.934	42.174	0.008	-8	-2	229
Midori-kawa	-32.648	-34.038	0.215	-32.589	-34.268	0.000	-59	230	215
Tamana-gum	-16.117	-39.454	-0.112	-16.184	-39.463	0.000	67	9	-112
Osuzu-yama	-77.347	40.425	1.480	-77.994	40.388	1.405	647	38	75
Kunimi-take	-50.584	2.061	1.661	-50.603	1.930	1.740	19	131	-79
Kyoto-yama	-47.268	-4.678	1.402	-46.999	-4.407	1.473	-269	-271	-71
Tsuno-minato	-83.173	54.196	-0.182	-83.104	54.201	0.000	-69	-5	-182

probably caused by misunderstanding of mountain top.

Also we have to remark that that the error of Z direction is under 200m. This tells us the possibility of making the photo-map of the scale 1:200000 with contour line directly from satellite photos.

Finally the position of satellite where photos were taken can be calculated from orientation element. And the following results were obtained:

st.1 X=-122.804km Y=-43,357km Z=443.411km

st.2 X=-72.922km Y=10.609km Z=443.629km

Brief report of an analyses of tidal current in Seto Inland Sea
by SKYLAB data

TAKAKAZU MARUYASU

May 31 1975

Brief report of an analyses of tidal current in Seto Inland Sea by SKYLAB Data

by Takakazu MARUYASU

The image taken from S190B of SKYLAB EREP pass in Jan. 11 1974 catchs the tidal current in Seto Inland Sea clearly. Seto Inland Sea is existed among Honshu, Shikoku and Kyushu land area and connected with the Pacific ocean through three channel ,Bungo,Kii and Naruto channel , and also with the Sea of Japan through the Kanmon channel. A number of islands is dotted on the Seto Inland Sea and this region is allocated as National Park. The scenery is very beautiful there. On the other hand the seaside there is almost developed as enormous industrial area recently. As the result the pollution by the drainaged water from industrial complex became serious environmental problem and the true effort to recover the past clear water has being held recently.

Seto Inland Sea as above mentioned is enclosed by the lands and slightly connected with the open sea through: 4 channels. By this reason the seawater stream is very complex and it is difficult to grasp the movement precisely. The goverment is trying to solve the phenomena by using the large model of Seto Inlans Sea but the analysed results are not clearly confirmed if the reproduced phenomena is true with fidelity.

S190B of EREP data presented the tidal stream clearly in a part of this region.

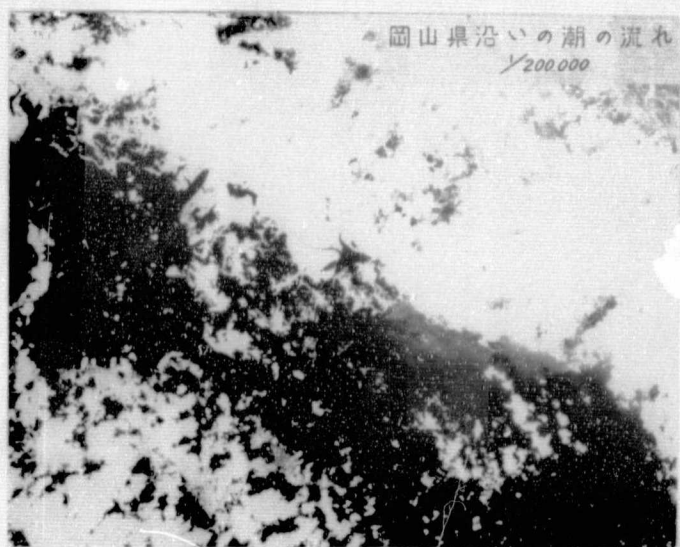


Fig-1 The tidal stream along the seaside of Okayama prefecture(by S190B)

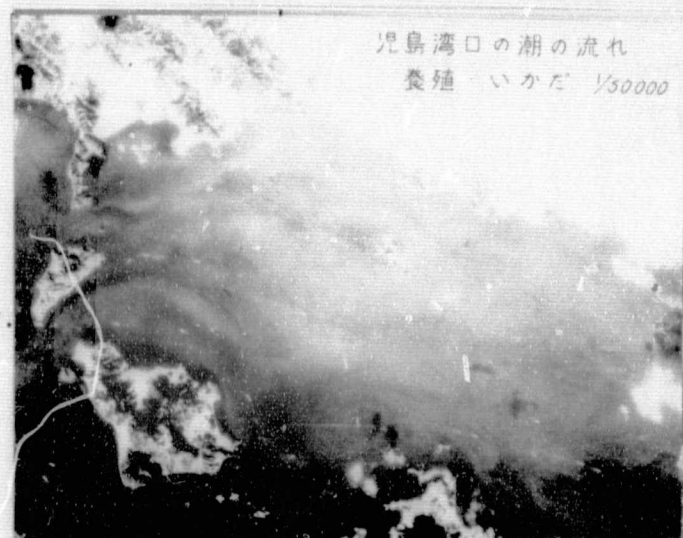


Fig-2 The tidal stream near the entrance of the Kojima bay (by S190B)

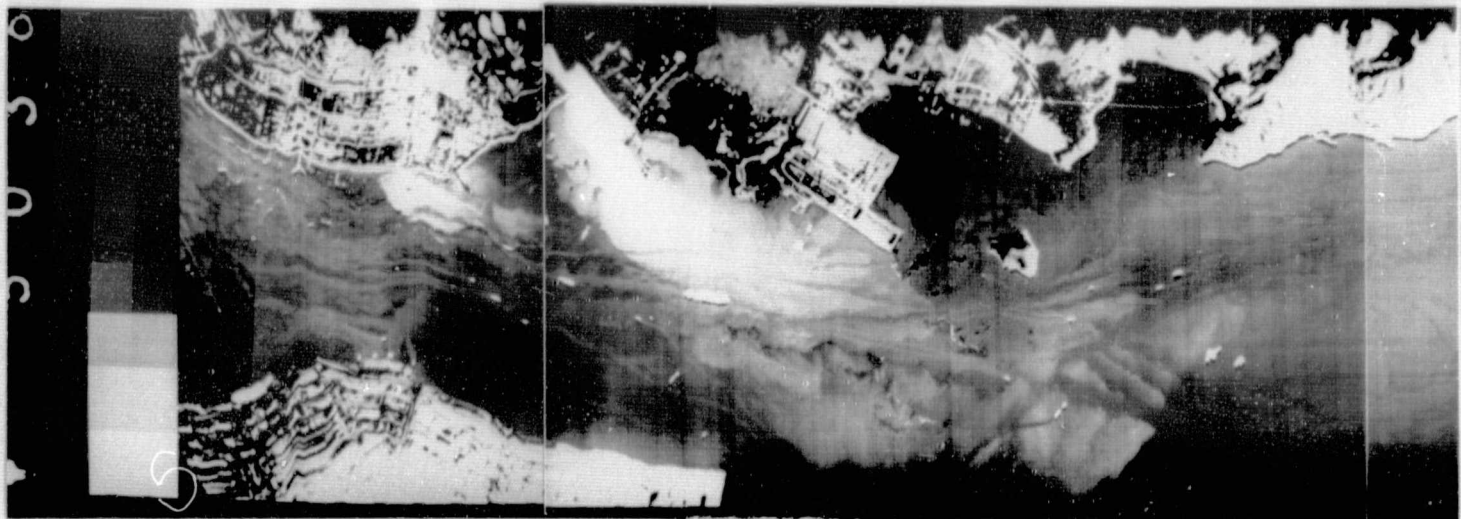


Fig-3 Mizushima oil spill pollution by Airborne Infrared Camera

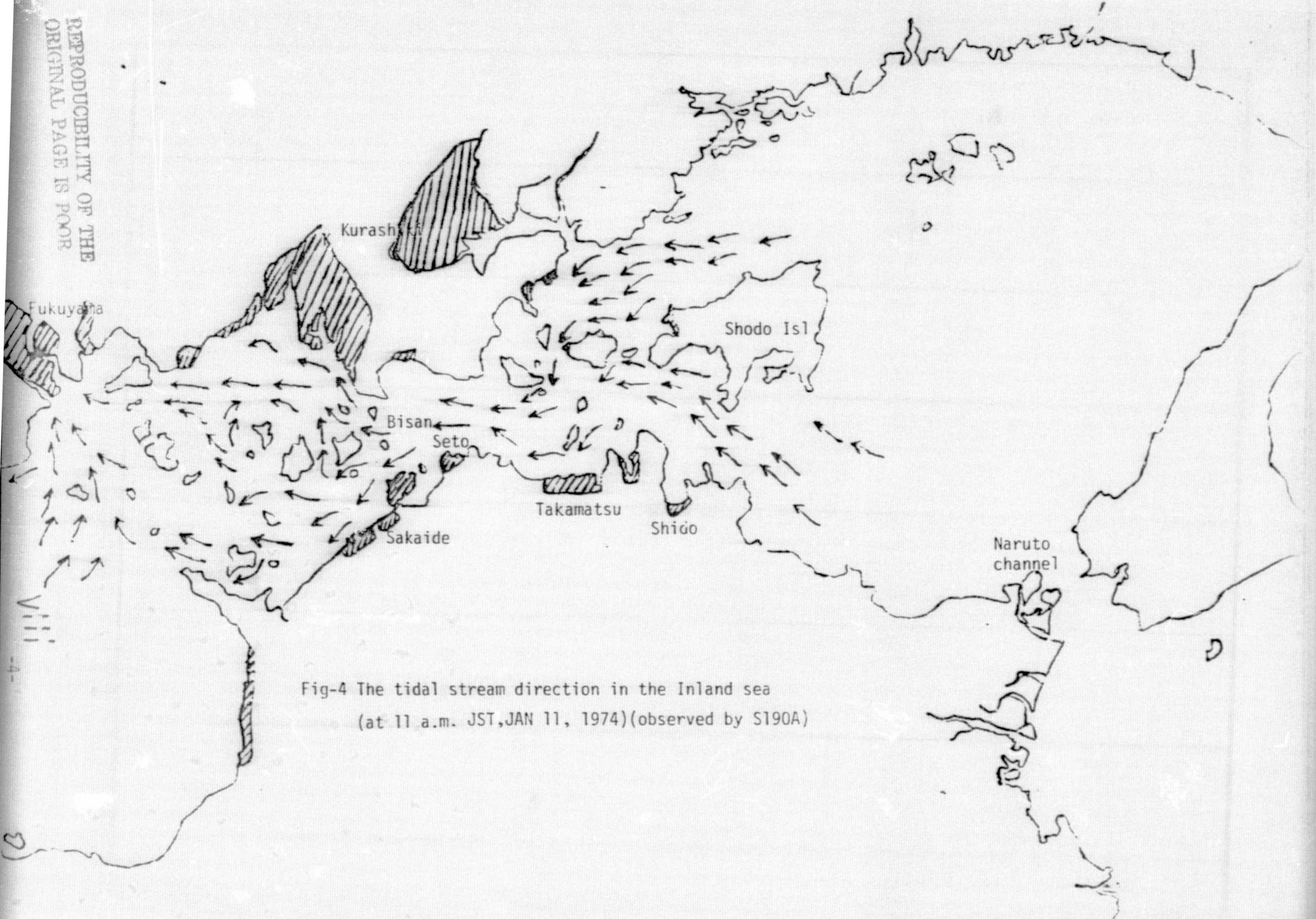
Occasionally the enormous oil spill accident was occurred in Mizushima industrial complex situated in the center of Seto Inland Sea in Dec. 1974. The accident was caused by the break of oil tank. The petroleum drifted toward east in Seto Inland Sea and reached till the Naruto cahannel. The stream direction was differed from one estimated before the accident, so experts recognized the complex phenomena of Seto Inland Sea renewally.

It was the time when the seasonal wind is very strong, then the movement of the floated petroleum on the watersurface is affected by wind therefore it could be said that the accident threw the new ploblem to solve the waterpollution in real.

The analyses of the photograph taken from SKYLAB station is executed about only a scene, so this result is not the solution of rises and falls of tidal current but it is clear that the photograph exhibits the complex stream line among the islands very visibly.

I heared that the cruising ships are too much in Seto Inland Sea. In the photograph the ships are obserbed likely as flying fishes. Additionally the scene of laver breeding bed is appeäred front of the Okayama beach clearly.

In this report the condition of oil spill photographed by the thermal sensor in the same time after a year as SKYLAB mission is showed in fig-3. The comparison



of two data will become the effective reference to solve the problem in Seto Inland Sea in future. And also the ERTS photograph catching the waterstream up to the Osaka bay through Kii channel is presented in this report.

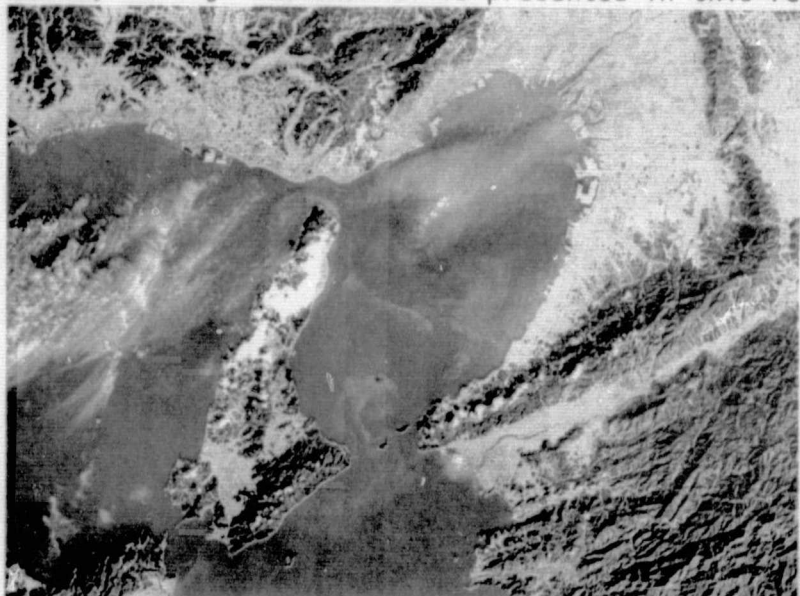


Fig-5 A current eddy, southwest of Osaka bay (by ERTS)

REPRODUCIBILITY OF THE
ORIGINAL PAGE IS POOR

Application of SKYLAB imagery to Marine
Environment around Japan

Hiroaki OCHIAI
Toba Merchant Marine College, Toba, Japan

Abstract

The application of space data is rapidly increasing in investigation and monitoring the marine environment. In this report, the author stressed capability of SKYLAB imagery as a index of remote sensing. Application of airborne data was also investigated.

1 Introduction

The objectives of this SKYLAB study were to analyze pollution, red tide, coastal current, sea ice and sea fog around Japan. During SKYLAB overpasses, airborne and sea truth data were collected. On January 11, 1973, SKYLAB-4 passed over the test site, Seto Inland Sea showed in Figure 1 and various kind of data were collected.

Although almost EREP data were distributed and investigated, S-192 MSS data were not yet analyzed.

2 Aircraft and Instrument

We tried special observation flight with twin engined aircraft showed in Figure 2 which have the capability of six hours flight equiped multi spectral scanner.

Our study group have a infrared scanner, five channels multi spectral scanner JSCAN-AT 5M and twelve channels multi spectral scanner which have a wavelength from UV channel to thermal channel.

For the purpose of to get the thermal profile of sea surface we always use PRT-5 and Matsushita's infrared thermometer.



Figure 1 SKYLAB pass 25 Track 49

REPRODUCIBILITY OF THE
ORIGINAL PAGE IS POOR



Figure 2 Observation aircraft.

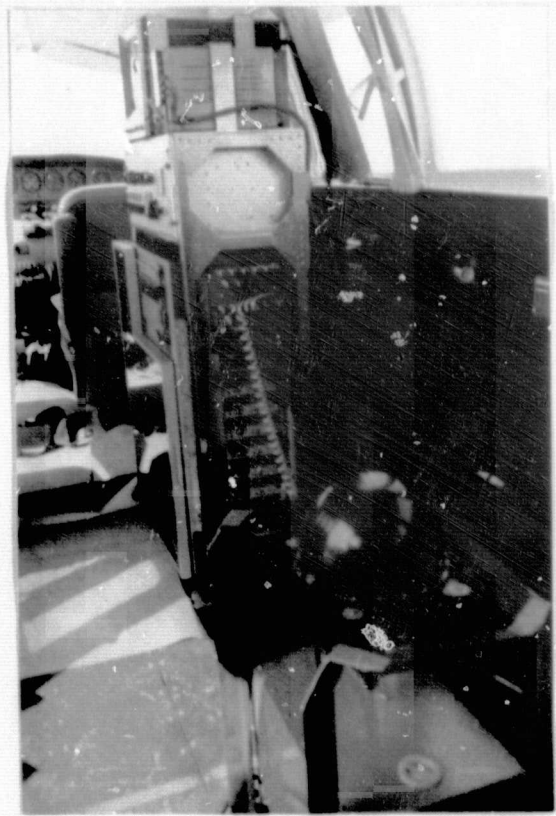


Figure 3 Multi spectral scanner.

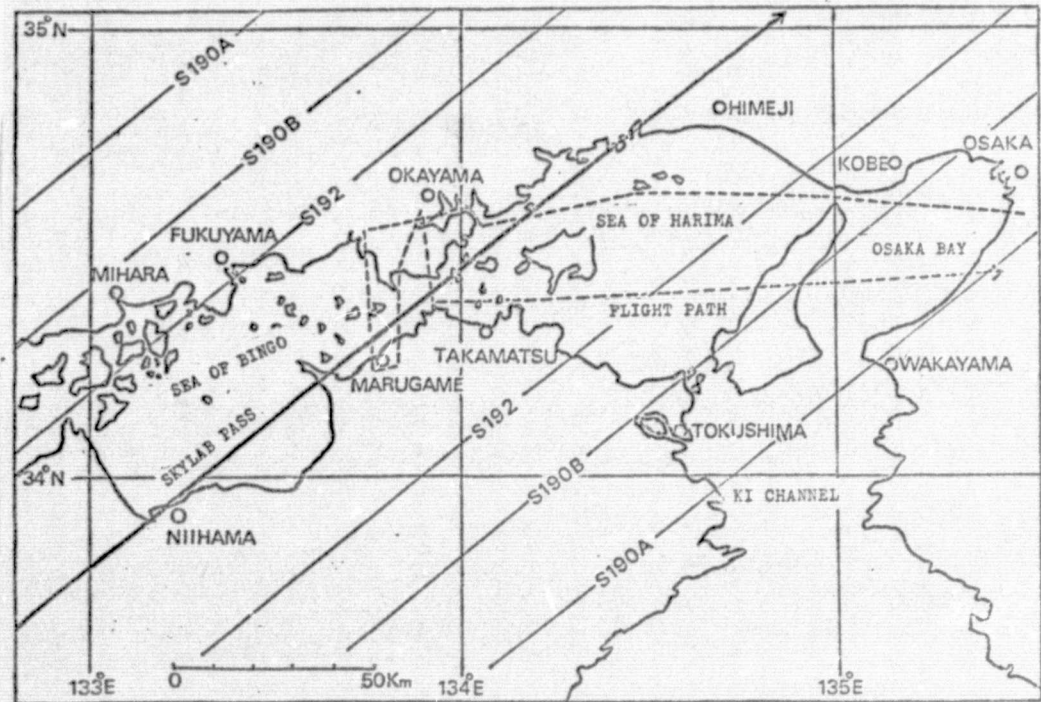


Figure 4 SKYLAB pass and flight path.

3 Seto Inland Sea Experiment

When the SKYLAB-4 passed along the track 49 on January 11, 1973, we tried special observation around the Seto Inland Sea using aircraft and ships and some investigations were carried out from the remote sensed data by SKYLAB and aircraft. The track 49 and flight paths of aircraft were shown in Figure 4.

3-1 Thermal distribution of sea surface

Enlarged S-190B photograph showed in Figure 5 shows the location of Mizushima and Sakaide area. Mizushima is very famous as one of the representative kombinat in Japan, especially in the field of oil refinery and iron manufacturing. So, from each factories a large amount of hot industrial effluent have been discharging.

In this area, sea water was so polluted that, fish coated by unfragrant smell was caught very often through the year and fragrant fish was estimated as a example of thermal pollution.

The investigation of the boundary of industrial effluent is very important around the coastal industrial zone. Figure 6 shows the thermal distribution of Mizushima kombinat. Hot efflux from oil refinery and iron manufacture were detected in detail. Around the Sakaide area we could find out the typical pattern of hot efflux from a power station clearly in Figure 7.

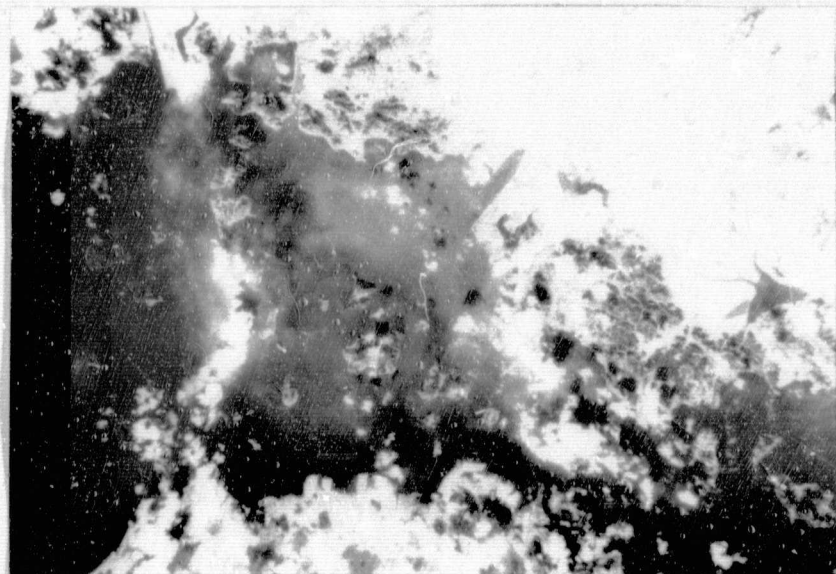


Figure 5 Enlarged S-190B photograph around the sea of Mizushima.

REPRODUCIBILITY OF THIS
ORIGINAL PAGE IS POOR



Figure 6 Infrared imagery around Mizushima area.



Figure 7 Infrared imagery around Sakaide area.

3-2 Pollution

Enlarged S-190B photograph around the southern part of the sea of Bingo showed in Figure 8 shows a oil pollution from a ship under going. Along the coast line a striped pattern was indicated.

It was estimated as the pattern of polluted bilge water from a ship and this pattern was not detected in any type photograph obtained by S-190A sensors.

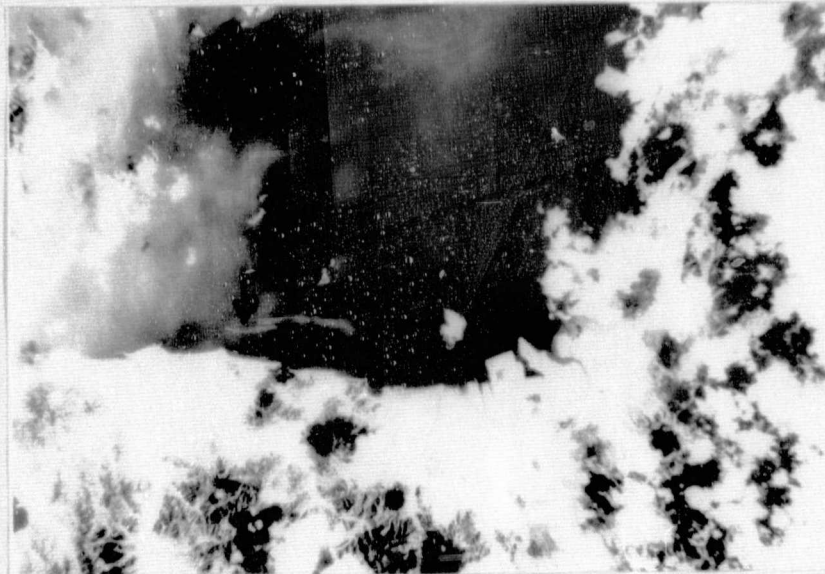


Figure 8 Enlarged S-190B photograph.

In S-190A color photograph showed in Figure 9, we could find out a black pattern in Osaka bay and this pattern was estimated as the boundary of industrial sedimentation spread on sea bottom.

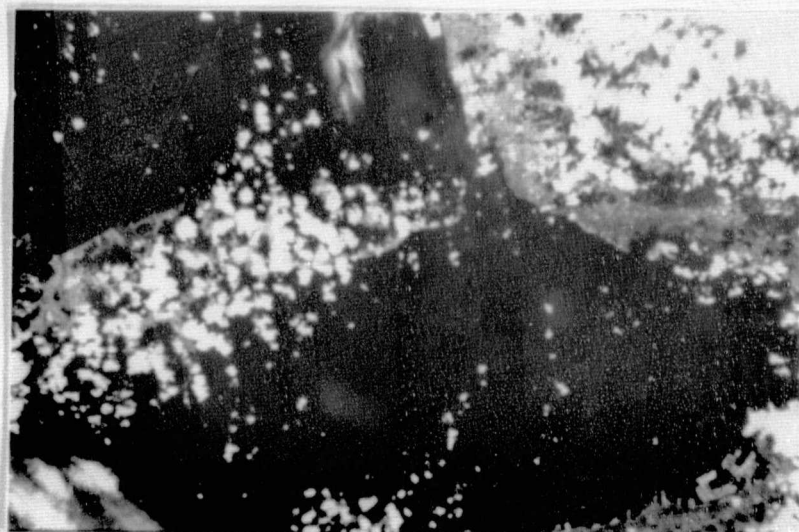


Figure 9 S-190A color photograph

3-3 Red tide

Depend on the increasing of industrial effluence from coastal industrial zone around the Kinki, Chugoku, Shikoku and Kyushu districts where newly developed kombinat like as Sakai, Takasago, Mizushima, Tkuyama, Ube, Sakaide, Niihama and Ooita were situated, the Seto Inland Sea was rapidly polluted and the environment of it was seriously bad condition now.

By the progress of red tide occurrence in the Seto Inland Sea showed in Table 1, in 1950, just one quater century ago, red tide occured only few cases for a year and the earea were restricted in Osaka bay and Hiroshima bay in warm season. We have not experienced in winter. But recently red tide occured in almost area of the Seto Inland Sea through the year.

For example, when SKYLAB passed over the Seto Inland Sea on January 11, 1973, we sighted red tide in the sea of Harima and in the sea of Bingo from the observation aircraft.

Table 1 The history of red tide occurrence in Seto Inland Sea

Year	Area	Scale
1950	Osaka bay Hiroshima bay	Small
1955	The sea of Hiuchi Hiroshima bay	Middle
1956	Tokuyama bay The sea of Suho The sea of Hiuchi	Large
1965	Almost area from The sea of Harima to The sea of Hiuchi Beppu bay Uwajima bay Saheki bay	Large
1970	Almost area of Seto Inland Sea	Large and dense
1972	The sea of Harima	Large and dense
1975	Almost area of Seto Inland Sea especially in Osaka bay and The sea of Harima	Large and dense

In 1972, fishing farm around the Ieshima islands in the sea of Harima were suffured by a large scale red tide many time and more than 140,000 fishs under farming were diseased.

The total damage of fishing farm was estimated more than 24 million dollers. So, the monitoring of the red tide is considered as the most important task for fishery. The yellow colored voltex showed in Figure 10 is one of red tide pattern we sighted in the sea of Bingo during the observation flight on January 11, 1973 and we could find it in enlarged S-190B photograph obtained by SKYLAB.

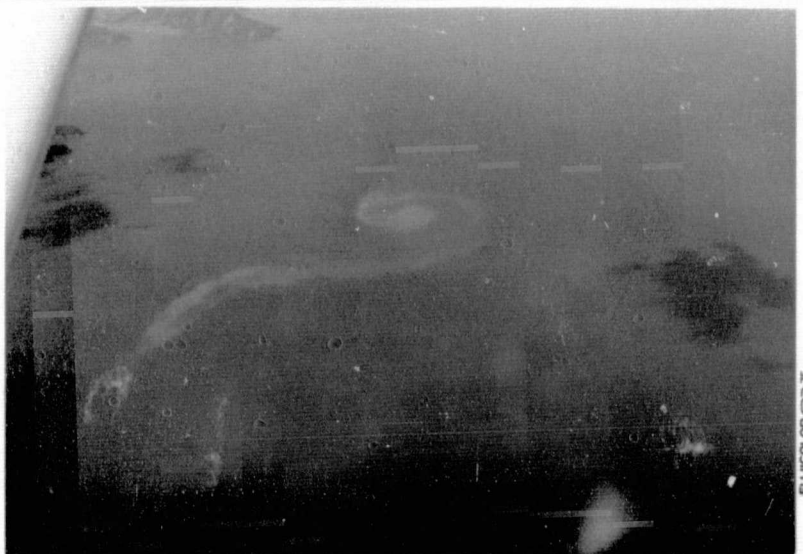


Figure 10 Aerial photograph of red tide.



Figure 11 Enlarged S-190B photograph around the sea of Bingo.

In Figure 11, we could find out another voltex in detail and it was also estimated as a typical red tide pattern occurred in narrow channel. These red tide pattern detected in S-190B photograph were not detected in S-190A any type photograph.

So we could say that only S-190B sensor was useful for the monitoring of red tide in small scale.

For the purpose of inquiry about the selection of the most effective wavelength of multi spectral scanner for the monitoring of red tide, we tried several observations with the technique of air-borne remote sensing in the sea of Harima and the sea of Bingo in 1973, 1974 and 1975. Figure 12 shows a example of red tide occurred in the sea of Harima, near Shodo island. Red stripes means distribution of Noctilca, typical red tide.

Although the occurrence mechanizm of red tide was not yet investigated clearly, we found that there are any correlation between the temperature distributions of surface water and abnormal growth of plankton. Figure 13 shows multi spectral imageries obtained by JSCAN-AT 5M multi spectral scanner which developed by our study group.

On comparison of five channel imageries, we could not find out so much difference in blue, green, orange and near-infrared imagery. But detected pattern in thermal imagery was quite different with another four imageries. We understood that the most effective wavelength for the monitoring of red tide is thermal channel.

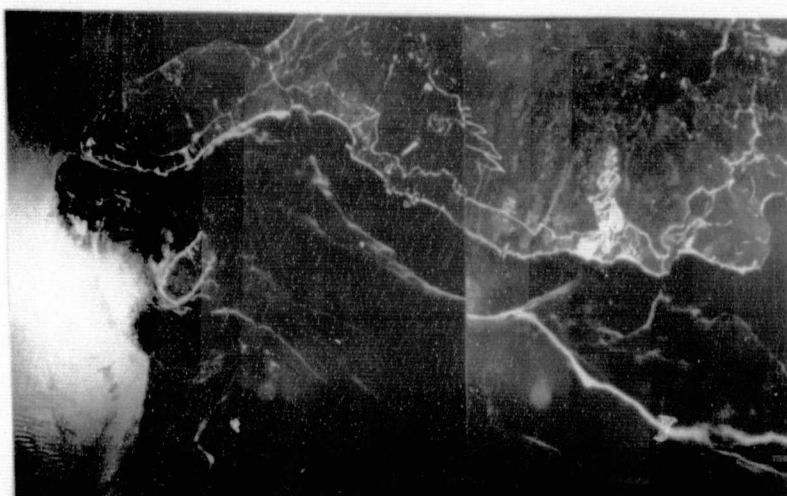


Figure 12 Mosaic of aerial photograph over red tide area.

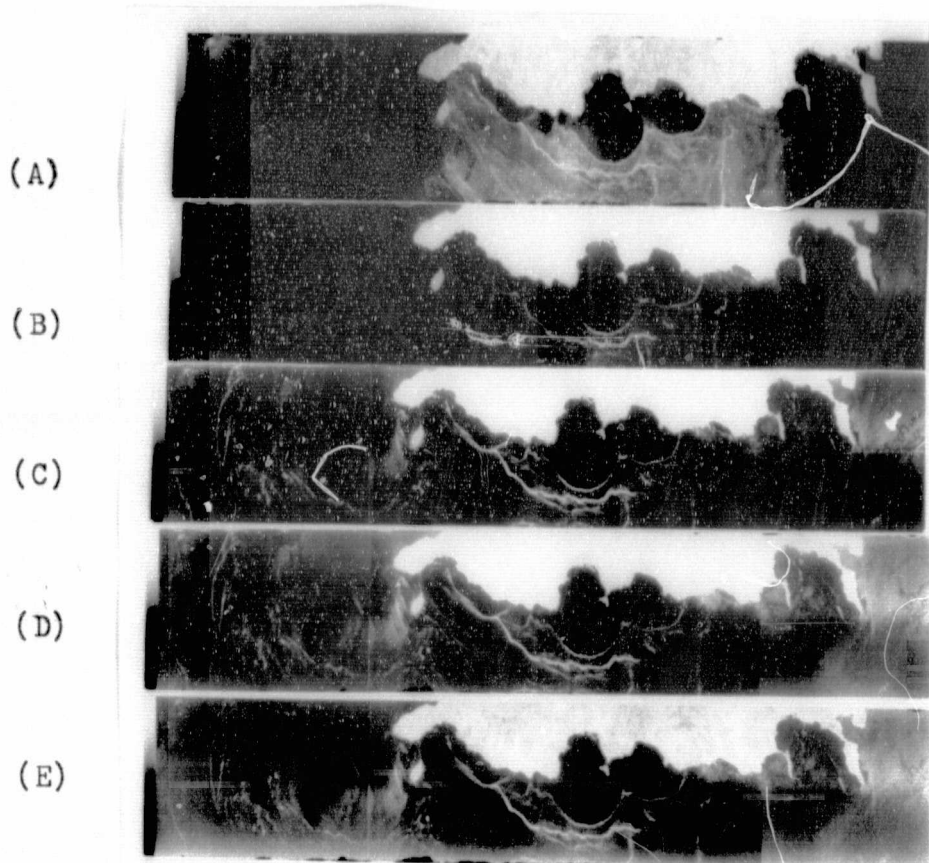


Figure 13 Multi spectral imageries.

- (A) Thermal band imagery
- (B) Near infrared imagery
- (C) Orange band imagery
- (D) Green band imagery
- (E) Blue band imagery

REPRODUCIBILITY OF THE
ORIGINAL PAGE IS POOR

4 Oceanic environment around Japan

Without the EREP Sensors SKYLAB has various kind of handy camera which was operated by astronaut and obtained photograph were very useful for the monitoring of oceanic environment. We analyzed several phenomena using 70mm and 35mm photograph.

4-1 Sea fog

The boundary of sea fog had been estimated with the data obtained by weather satellite. But it was not so exactly compared with SKYLAB data. Figure 14 shows the boundary of sea fog around the sea of Okhotsk. In this photograph the cloud formation was also indicated clearly. We could understand that sea fog occurred in the sea of Okhotsk and extends toward the northwest direction. Beyond the coast line of southern Sakhalin sea fog extended considerably. Around the coast line of northeast Hokkaido and Soya strait, sea fog was not extended and it depended on the wind direction.

Figure 15 shows dynamic pattern of sea fog near the Kurie islands. Cloud streak was caused by island interrupting and these cloud formation was called Von Jarnan vortex. Oppositely curving pattern were delightful.

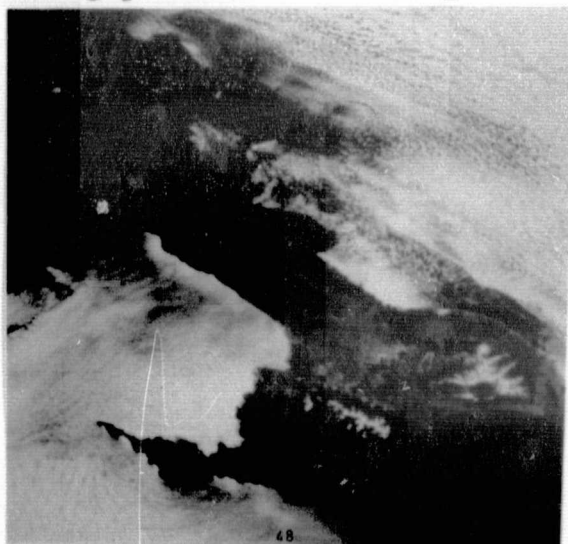


Figure 14 Sea fog over the sea of Okhotsk.

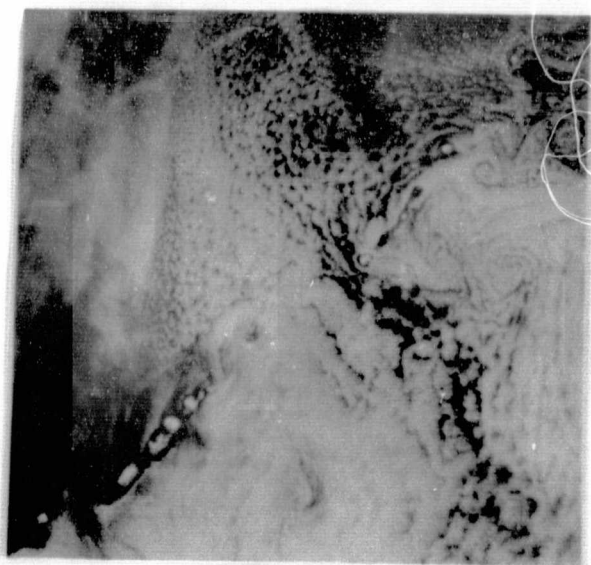


Figure 15 Fantastic cloud formation of sea fog.

4-2 Sea ice

During the winter the sea of Okhotsk was frozen caused by drifting ice from the northwest part of the sea of Okhotsk and the monitoring of the drifting ice along the northeast coast of Hokkaido is very important not only fishery but also estimation of climate. So, three radar sites were arranged at Esashi, Monbetsu and Abashiri for purpose of the monitoring of sea ice.

The maximum range were showed in Figure 16. All maximum range were below 100 kilometers. Compared with radar faculty LANDSAT(ERTS) performs effectively in the boundary of monitoring.

LANDSAT imagery showed in Figure 17 is one of the example of drifting ice in the sea of Okhotsk. But 70mm photograph obtained by SKYLAB showed in Figure 18 is more useful for the monitoring sea ice. In this photograph we could find out all informations between Soya strait and Kunashiri strait. For example, distinct formation of drifting ice were carried out.

The boundary of fast ice along the coast of Hokkaido was also investigated. Figure 19 and Figure 20 shows the effect of coastal current which disturb the direction of drifting ice.

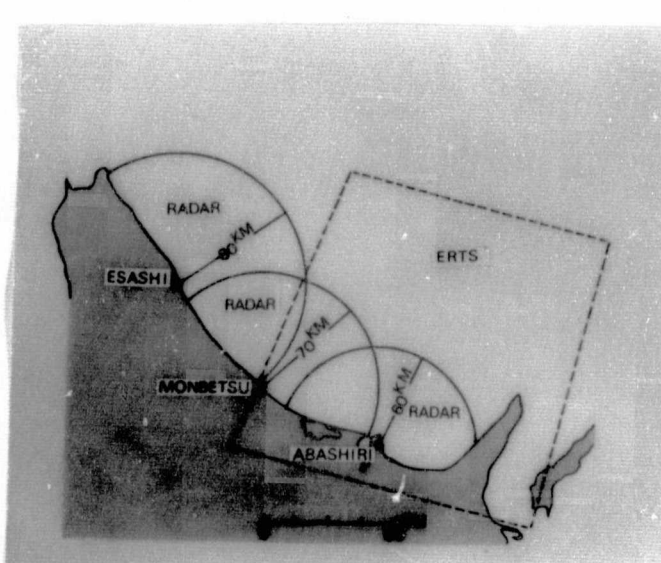


Figure 16 Location of radar site.

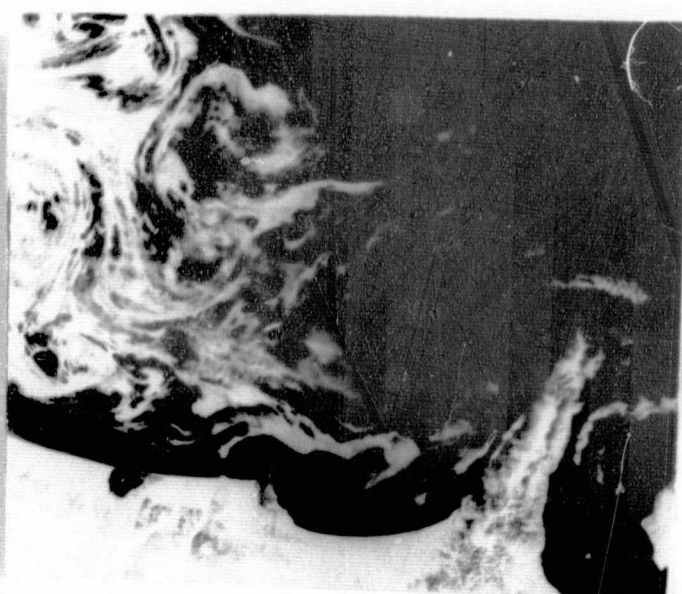
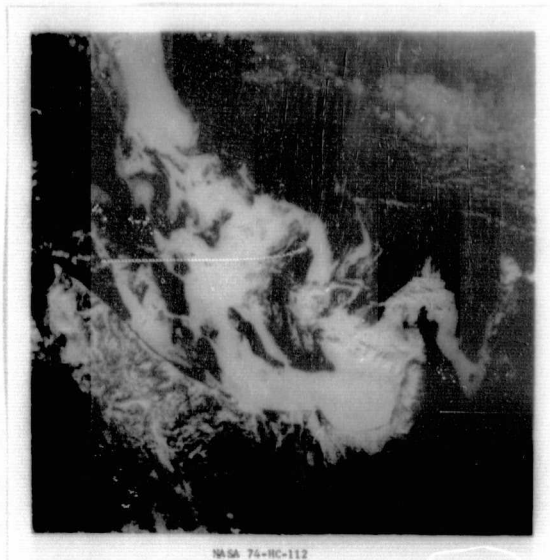


Figure 17 LANDSAT imagery.



NASA 75-HC-112

Figure 18 70mm photograph obtained by SKYLAB.

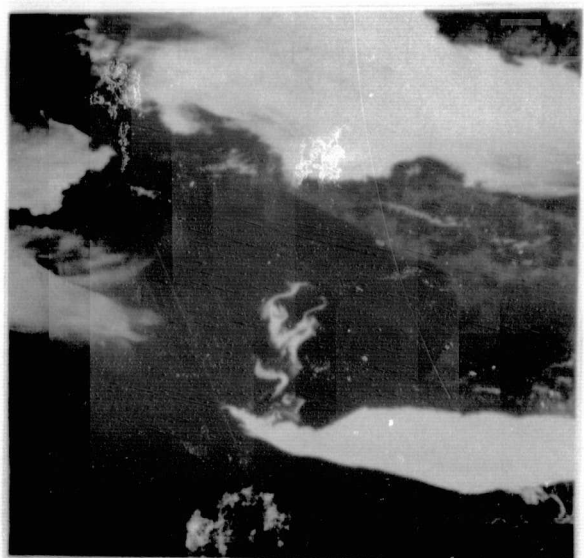


Figure 19 Typical pattern of drifting ice.



Figure 20 Close up of drifting ice indicated in Figure 19 obtained by 35mm camera(Nikon).

REPRODUCIBILITY OF THE
ORIGINAL PAGE IS POOR

5. Conclusions

High resolution data obtained by EREP sensor were very useful for investigation of marine environment, especially monitoring of coastal phenomena in aspect of environmental quality studies. In this respect, the digital analyses of S-192 MSS data would proved particularly important.

METHODOLOGICAL CONSIDERATIONS ON SPACE PHOTO-
INTERPRETATION FOR ENVIRONMENTAL STUDIES

by Takamasa NAKANO, Tokyo Metropolitan
University, Japan

I INTRODUCTION

In order to examine the possibility and the limitation of space photo-interpretation for environmental studies, ERTS I(LANDSAT I), SKYLAB Photos, various types of aerial photos and the ordinary topical maps on natural environment of the same areas have been comparatively studied.

As the test areas, Kagoshima Prefecture, southernmost part of Kyushu, and Tokyo district were selected. The former area is well photographed from SKYLAB and is rather underdeveloped, rather environmentally preserved and simply structured geomorphologically. The latter area is most intensively inhabited and badly urbanized, and many attempts have been conducted by many specialists using various modern instruments and many instructive results have been brought out.

Both areas are covered with various maps such as landform, lithology, soil, land use, vegetation and land capability on scales from 50,000 to 500,000. Besides, various types of aerial photos taken in different seasons mostly at large or medium scales are available, particularly in Tokyo area. Unfortunately, however, small scale photos are not available.

2 METHODS

Various methods such as social scientific, psychological, historical, geographical, geophysical, geochemical, geological and other methods based on different disciplines have been applied for environmental studies. Technically, those methods are classified into several categories. Documentational, juristical, statistical, computational, cartographical, observational, photographic, image processing methods are now commonly used. In this study, carto-

graphical and traditional photo-interpretation technics are applied.

I) Space photos are examined in forms of prints and or films of various types independently prepared. Ordinary photo-interpretation technics are major concerns and various types of instrumental treatments are not applied for this study, except the use of the results of instrumental treatments carried out by other specialists.

2) For comparison with SKYLAB photos in January 1974, two stations for infra-red photography were set up in and out of Tokyo at the tops of buildings over 40 meter in height. Unfortunately, however, SKYLAB photos were not taken. Thermal photos of Tokyo area in August 1973 were also out of use, because of no SKYLAB data available. On the latter, short report is published in TOSHIKENKYU HOKOKU (Reports on Urban Studies) of Tokyo Metropolitan University in Japanese.

3) For detail examination of the results on LANDSAT I by means of various instrumental analyses, statistics on land use, housing, buildings etc. were checked.

3 RESULTS

I) It is clear that the SKYLAB photos of geographically not so well known areas can provide valuable informations, particularly on land use, vegetation, geological structure, landform, soil pattern etc.

In order to examine the quality of SKYLAB films of the area of Kagoshima Prefecture, films of separate bands, color and false color, were independently projected onto the maps on landform, lithology, soil and land use. By this test it is understood that if some data at patched spots in the area concerned are available, reconnaissance maps on those items can be compiled. But, if no reliable data available, maps on those items are poorly compiled (Table I).

2) However, attention should be drawn to that the space data by means of instrumental analyses are not always basing on the previously known concepts on the informations in various maps. On the systematization of space-borne data and interpretation to or correlation with the previous scientific concepts, further efforts and data accumulation are necessary.

3) Although no SKYLAB photos are available, LANDSAT I photos provided by various methods are reexamined to systematize the terrestrial, air and space-borne data. For instance, according to a Japanese report on urbanization and environmental changes, high buildings cover 20%, low houses 50%, open space 8%, roads and railways 20%, etc. However, no statistical data support those figures. Brief comments on famous LANDSAT I photo of Tokyo area dealing such problems will be published in NEU ENTDECKUNG DER ERDE.

4) On the other hand, if the interpreter is familiar with the test area, it is sure that various topical maps on land use, landform, geology, soil, vegetation are easily and preliminary compiled, particularly on composited color enlarged prints.

5) In Japan, high altitude photography and photo-interpretation of such smaller scale photos are not so often experienced. So far as the author understands, such experiences are fundamentally necessary for better application of space-borne data for environmental studies.

Table 1 Interpretability of SKYLAB photos, LANDSAT I photos and air photos

Remarks; This test was carried out by two operators, and one of them has no experience on space photo-interpretation. Generally speaking, space photos can provide useful informations on environments and necessary topical maps will be prepared by means of space photo-interpretation.

A: Items to be analysed are selected from published land classification maps on scale of 1:200,000.

B: Various types of aerial photos on medium scales. No reference data used.

C: LANDSAT 1 prints, ca 1:1 million scale, various types of composited images.

D: SKYLAB color film E: SKYLAB infra-red color film F: SKYLAB Band 6.

y: yes n: no ?: doubtful -: no check y-n: partly yes, partly no.

A	B	C	D	E	F
a MOUNTAIN LAND					
1 Relative height, more than 600 m	y	y	y	y	y
2 " , 400-600 m	y-n	n	n	n	n
3 " , 200-400 m	y-n	n	n	n	n
4 Piedmont slope, less than 200 m	y-n	n	n	n	n
b VOLCANIC LAND					
5 Relative height, more than 600 m	y-n	y-n	y-n	y-n	y-n
6 " , 400-600 m	y-n	n	n	n	n
7 " , 200-400 m	y-n	n	n	n	n
8 Volcanic flank, less than 200 m	y-n	y-n	y-n	y-n	y-n
9 Lava plateau	y-n	y-n	y-n	y-n	y-n
10 Volcanic detritus covered area	y-n	y-n	y-n	y-n	y-n
11 Welded tuff area	n	n	n	n	n
12 Crater, caldera wall	y	y	y	y	y
c HILL LAND					
13 Relative height, 100-200 m	y	y	y	y	y
14 " , less than 100 m	y-n	y-n	y-n	y-n	y-n
d FLAT LAND					
15 Rock terrace	y	y	y	y	y
16 Gravel terrace	n	n	n	n	n
17 Limestone plateau	n	n	n	n	n
18 Fan	y-n	y-n	y-n	y-n	y-n
19 Delta	y	y	y	y	y
20 Natural levee, sand bar, sand dune	y	y	y	y	y
21 Former river course	y	y-n	y-n	y-n	y-n
22 Artificial land	y	y-n	y-n	y-n	y-n
e COAST					
23 Tidal flat, beach	y	y	y	y	y
24 Drift sand	y	y-n	y-n	y-n	y-n
25 Dirty water	y-n	y-n	y-n	y-n	y-n
26 Fresh water	y-n	y-n	y-n	y-n	y-n
27 Coral reef	y	-	-	-	-
f GEOLOGY	to be inferred from landform features				
28 Alluvium	y	y	y	y	y
29 Diluvium	y	y	y	y	y
30 Younger complexes	y	y	y	y	y
31 Older complexes	y	y	y	y	y
32 Fault	y	y	y	y	y
33 Lineament, various origins	y	y	y	y	y

	to be inferred from landform features				
g SOIL					
34 Lithosols	y	y	y	y	y
35 Sand dune soil	y	y	y	y	y
36 Ando soil (black soil)	y-n	y-n	y-n	y-n	y-n
37 Brown forest soil	-	-	-	-	-
38 Reddish yellow soil	n	n	n	n	n
39 Grey lowland soil	?	?	?	?	?
40 Paddy field soil	y	y	y	y	y
41 Peat bog soil	y-n	y-n	y-n	y-n	y-n
h LAND USE	generally interpretable				
42 Paddy field	y	y	y	y	y
43 Dry field	y	y	y	y	y
44 Orchard, tea garden	y	y	y	y	y
45 Urban structure	y	y-n	y-n	y-n	y-n
45 CBD	y	y-n	y-n	y-n	y-n
46 Industrial area	y	y-n	y-n	y-n	y-n
47 Air field	y	y	y	y	y
48 Dammed lake	y	y	y	y	y
49 Major road	y	y-n	y-n	y-n	y-n
50 Railway	y	y-n	y-n	y-n	y-n